Inorganic Chemistry

Article

pubs.acs.org/IC

High-Pressure Polymorph of Phosphorus Nitride Imide HP_4N_7 Representing a New Framework Topology

Dominik Baumann and Wolfgang Schnick*

Department of Chemistry, University of Munich (LMU), Butenandtstrasse 5−13, 81377 Munich, Germany

Supporting Information

ABSTRACT: A new polymorph of phosphorus nitride imide HP_4N_7 has been synthesized under high-pressure/high-temperature conditions from P_3N_5 and NH_4Cl at 6 GPa and temperatures between 800 and 1300 °C. Its crystal structure was elucidated using single-crystal X-ray diffraction data. β-HP_4N_7 (space group $C2/c$, no. 15, Z = 4, a = 12.873(2) Å, b = 4.6587(4) Å, c = 8.3222(8) Å, β = 102.351(3)°, R_1 = 0.0485, wR_2 = 0.1083) crystallizes in a new framework structure type that is made up of all-side vertex-sharing PN_4 tetrahedra. The topology of the network is represented by the point symbol $(3^2.4^2.5^2.6^3.7)(3^4.4^4.5^4.6^3)$, and it has not been identified in other compounds so far. Structural differences between the two polymorphs of HP_4N_7 as well as the topological relationship to the recently discovered high-pressure polymorph β-HPN_2 are discussed. Additionally, FTIR and solid-state NMR spectroscopy are used to corroborate the results of the structure determination.

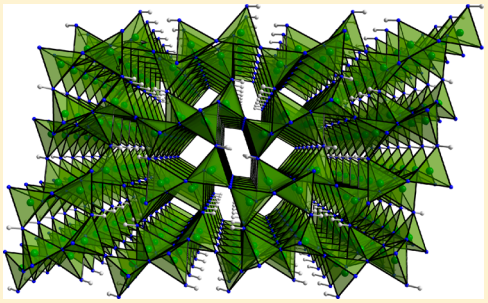

INTRODUCTION

Compounds that comprise tetrahedral framework structures are of high interest both from a scientific point of view and concerning their broad technical applicability. Archetypical tetrahedral framework structures are formed by silicates and related compounds such as alumosilicates or alumophosphates.[1,2] Prominent applications of such materials include sorption and catalysis in the case of zeolites[3] as well as optical materials and piezoelectrics, particularly in the case of quartz.[4] Properties of these functional materials are intrinsically facilitated by their respective crystal structures. Accordingly, the discovery of new tetrahedral framework structures both with new topologies or new elemental compositions is an important issue for material scientists.[4]

The emerging interest in nitridosilicates during the past few years can in part be attributed to their broad structural variety as well as their high chemical and thermal stability. The latter qualities stem from the inclusion of the nitride ion N^{3-}, which in nitridosilicates can link up to four tetrahedral centers as opposed to two in the case of oxosilicates.[5] Undoubtedly, this structural variability expands greatly the range of possible crystal structures and furthermore allows higher degrees of condensation than would be possible in oxosilicates. In recent years we could show that the substance class of (oxo)-nitridophosphates rivals even the structural diversity of nitridosilicates. Silica analogous phosphorus oxonitride PON forms a high-pressure polymorph, the structure of which was predicted for SiO_2 but has never been observed.[6] Other representatives in this system include porous compounds such as the first nitridic zeolites NPO[7] and NPT[8] as well as the clathrate $P_4N_4(NH)_4(NH_3)$.[9] Glassy compounds in the system Li−Ca−P−N have displayed remarkable values for hardness and refractive index.[10] Existing applications of phosphorus nitrides such as PON and HPN_2 are mainly in the field of flame retardation.[11,12] Theoretically predicted cubic BeP_2N_4 is expected to show superior mechanical properties,[13] possibly making it a suitable material for high-performance tools. As these examples show, further research on new nitridophosphate frameworks is likely to lead to the discovery of novel compounds exhibiting interesting properties.

The synthesis of nitridophosphates can be markedly facilitated by the use of high-pressure techniques. On one hand, this approach allows suppression of thermal decomposition of the products, which occurs typically at high temperatures necessary for synthesis. On the other hand, according to the pressure-coordination rule,[14] very high pressures allow access to structures featuring higher coordination numbers,[15] one of the most prominent examples being the mineral stishovite.[16] In the case of phosphorus nitrides a higher coordination number of phosphorus has been realized in γ-P_3N_5, where two-thirds of the P atoms are coordinated by nitrogen in the form of a square pyramid.[17] An increase in coordination number often leads to a significantly increased hardness, making this type of compound interesting for material scientists.[15]

In this contribution we demonstrate the high structural flexibility of nitridophosphate frameworks by characterizing an entirely new topology realized in a high-pressure polymorph of phosphorus nitride imide β-HP_4N_7.

Received: April 1, 2014
Published: July 18, 2014

dx.doi.org/10.1021/ic500767f | Inorg. Chem. 2014, 53, 7977−7982

EXPERIMENTAL SECTION

Synthesis of P_3N_5. P_3N_5 was obtained by reaction of P_4S_{10} with dry ammonia gas according to the literature.[18] P_4S_{10} (8.0 g, 36 mmol, 99%, Sigma-Aldrich) was placed inside an open-ended silica glass tube (length 30 cm) that was inserted into a silica glass flow tube. The reactant was saturated with streaming dry ammonia (99.98%, Air Liquide) for 4 h at room temperature and subsequently heated to 850 °C for 8 h. After cooling, the brown reaction product was washed sequentially with deionized water, ethanol, and acetone.

Synthesis of β-HP_4N_7. β-HP_4N_7 was synthesized under high-pressure/high-temperature conditions in a modified Walker-type multianvil assembly using a 1000 ton hydraulic press (Voggenreiter, Mainleus, Germany). P_3N_5 (48 mg, 0.295 mmol) and NH_4Cl (4 mg, 0.075 mmol, 99.5%, Sigma-Aldrich) were thoroughly ground in an agate mortar, tightly packed into a cylindrical boron nitride crucible (Henze, Kempten, Germany), and centered in a 18/11 MgO octahedron. A detailed description of the assembly can be found in the literature.[19−23] The sample was compressed between eight truncated tungsten carbide cubes (Hawedia, Marklkofen, Germany) to a pressure of 6 GPa at room temperature during 164 min. It was subsequently heated to 800 °C during 15 min, held at this temperature for 240 min, and cooled to room temperature during 30 min. Finally, it was decompressed during 600 min. After isolation and grinding the sample was obtained as a light gray air-stable powder. Excess NH_4Cl was removed by washing the sample with deionized water, ethanol, and acetone. Single crystals suitable for X-ray diffraction were obtained by heating the reaction mixture to 1300 °C within 15 min, holding the temperature for 60 min, and cooling within 15 min.

Spectroscopic Analysis. The chemical composition of the sample was established by energy dispersive X-ray spectroscopy using a JSM 6500F scanning electron microscope (Jeol) with an Oxford Instruments 7418 Si/Li EDX detector. FTIR spectra were collected employing KBr disks with the use of an IFS 66 v/S spectrometer (Bruker). Solid-state MAS NMR experiments were carried out on an Avance III spectrometer (Bruker) at a field strength of 11.7 T with a 2.5 mm probe at a spinning rate of 20 kHz. ^1H and ^{31}P chemical shift values are referenced to 0.1% TMS in $CDCl_3$ (Sigma-Aldrich) as an external reference. Diffuse reflectance UV−vis spectroscopy was carried out on a Cary 500 spectrometer (Varian) equipped with a praying mantis diffuse reflectance accessory.

Crystal Structure Analysis. Single-crystal X-ray diffraction analysis was carried out on a Bruker D8 Quest diffractometer equipped with a microfocus X-ray source (Mo Kα radiation) at 140 K. A crystal of the size 0.035 × 0.065 × 0.070 mm^3 was chosen from the coarsely ground sample under paraffin oil. The crystal structure was solved *ab initio* using the charge-flipping algorithm as implemented in the program Superflip.[24−26] Subsequent full-matrix least-squares refinement was carried out on F^2 using SHELXL-97.[27] The position of the hydrogen site was extracted from difference Fourier maps. The N−H distance was restrained to 0.9 Å. Due to the low absorption coefficient and the very small crystal size, no absorption correction was applied. Powder X-ray diffraction data were collected in parafocusing Debye−Scherrer geometry on a Stadi P diffractometer (Stoe, Darmstadt, Germany) using Ge(111)-monochromated Cu Kα_1 radiation and a linear position sensitive detector. The ground sample was enclosed in a glass capillary (diameter 0.3 mm). Rietveld refinement was carried out using TOPAS-Academic 4.[28] The peak shape was modeled using the fundamental parameters approach (direct convolution of source emission profiles, axial instrument contributions, crystallite size, and microstrain effects).[29,30]

RESULTS AND DISCUSSION

Synthesis. As previously reported, the synthesis of phase-pure α-HP_4N_7 was accomplished with the use of the moisture-sensitive molecular precursor $(NH_2)_2P(S)NP(NH_2)_3$.[31] Under ambient pressure the simple reaction between phosphorus nitride and ammonium chloride (eq 1) does not yield a pure product.

$$4\ P_3N_5 + NH_4Cl \rightarrow 3\ HP_4N_7 + HCl \quad (1)$$

However, at high pressures this reaction proceeds cleanly and yields pure samples of β-HP_4N_7. This high-pressure polymorph can be synthesized in a multianvil assembly at pressures between 5 and 8 GPa at temperatures ranging from 750 to 1400 °C. Purest samples have been obtained at 750 °C with constant heating for 240 min. Higher reaction temperatures lead to the formation of significant amounts of side phases but promote crystal growth. Therefore, single crystals for structure determination were grown at 1300 °C, whereas bulk samples were synthesized at 800 °C. The purpose of using NH_4Cl in this synthesis is twofold. Primarily, it acts as reactant and H^+-donor. However, recently we have demonstrated that NH_4Cl functions as an effective mineralizer for the synthesis of nitridophosphates.[32] With this synthetic approach the product is obtained in the form of a gray sintered pellet that yields a light gray air-stable powder after grinding. Single crystals of β-HP_4N_7 form colorless platelets. An atomic ratio of P:N = 4:6.9 was determined by energy-dispersive X-ray (EDX) analysis, which is in good agreement with the sum formula HP_4N_7. Oxygen was detectable only in trace amounts in the sample.

Crystal Structure of β-HP_4N_7. The crystal structure of β-HP_4N_7 was determined from single-crystal X-ray diffraction data. The reflections were indexed with a monoclinic unit cell (a = 12.873(2) Å, b = 4.6587(4) Å, c = 8.3222(8) Å, β = 102.351(3)°).[33] Structure solution was performed assuming space group $C2/c$ (15), as indicated by the systematic absences. All heavy atom positions were determined during structure solution. The position of the hydrogen atom was unequivocally localized from difference Fourier maps during structure refinement. The single crystallographic hydrogen atom site leads to two adjacent positions in the unit cell coupled by an inversion center. Their respective distances indicate a mutually exclusive occupation, represented by a fixed occupation factor of 0.5 during structure refinement. Due to the small diffraction contribution of hydrogen, it cannot be decided whether a symmetry reduction (loss of centrosymmetry toward Cc) leading to an ordered structure model with respect to the hydrogen atoms is required. Crystallographic data for β-HP_4N_7 are summarized in Table 1. Details on the atomic positions as well as selected bond lengths and angles are listed in Tables 2 and 3, respectively.

The crystal structure of β-HP_4N_7 (Figure 1) consists of a three-dimensional network of all-side vertex-sharing PN_4 tetrahedra. In contrast to the ambient pressure modification there are no edge-sharing tetrahedra. The framework is characterized by the existence of 3-, 4-, and 5-rings. The six-membered rings are large enough to provide space for the single hydrogen atom, which is covalently bound to half of the nitrogen atoms pointing into the ring.

Figure 2 illustrates the coordination of the atoms in β-HP_4N_7. Both P atoms are coordinated tetrahedrally by nitrogen, with bond angles P−N−P of 103.7(1)−120.8(2)°, slightly deviating from the regular tetrahedral angle. The N bridges are linking either two or three PN_4 tetrahedra, respectively. The position of the H atoms is corroborated by the fact that P−N bonds around the protonated N2 are significantly longer than those of the unprotonated N1 and N3. Bond lengths around the triply coordinating N4 are even larger, ranging from 1.682(2) to 1.739(2) Å, which is consistent with the values observed in other nitridophosphates such as α-HP_4N_7 or MP_4N_7 (M = Na, K, Rb, Cs).[34] The bond angles

dx.doi.org/10.1021/ic500767f | Inorg. Chem. 2014, 53, 7977−7982

Table 1. Crystallographic Data and Details of the Structure Refinement for β-HP_4N_7

cryst size/mm^3	0.035 × 0.065 × 0.070
molar mass/g·mol^{-1}	222.96
cryst syst	monoclinic
space group	$C2/c$ (no. 15)
T/K	140(2)
radiation, λ/pm	Mo Kα, 71.073
a/Å	12.873(2)
b/Å	4.6587(4)
c/Å	8.3222(8)
β/deg	102.351(3)
V/Å^3	487.55(8)
Z	4
calcd density/g·cm^{-3}	3.037
absorp coeff/mm^{-1}	1.459
measd reflns	8803
indep reflns	1218
obsd reflns	909
refined params	55
GOF	1.046
final R indices [$I > 2\sigma(I)$]	$R_1 = 0.0485$; $wR_2 = 0.0984^a$
final R indices (all data)	$R_1 = 0.0769$; $wR_2 = 0.1083^a$

$^a w = 1/[\sigma^2(F_o^2) + (0.0458P)^2 + 2.3837P]$, with $P = (F_o^2 + 2F_c^2)/3$.

around N4 are very close to 120°, which is indicative of an almost regular trigonal planar coordination. In contrast to α-HP_4N_7 no edge sharing of tetrahedra occurs in this framework. Nevertheless, the phase transition leads to an increase in density of 6.0%. Therefore, the increase of density due to the tilting of the tetrahedra offsets the loss of shared tetrahedra edges and leads to an overall higher density of β-HP_4N_7. This difference in densities stabilizes this crystal structure at high pressures.

In order to characterize the framework topology of the network, the point symbol $\{3^2.4^2.5^2.6^3.7\}\{3^4.4^4.5^4.6^3\}$ was calculated by the program TOPOS.[35,36] This network topology is distinct from that of α-HP_4N_7, the isosteric P_4N_6O,[37] and the related nitridophosphates MP_4N_7 (M = Na, K, Rb, Cs)[34] and has in fact not been observed in any compound so far. The change in topology also indicates that the transition from α-HP_4N_7 to β-HP_4N_7 is reconstructive. It has been illustrated in the past that the structure of ambient-pressure HP_4N_7 can be derived from the structure of less condensed α-HPN_2. This process involves formal release of NH_3 and the simultaneous formation of new P−N−P linkages. Analogously, Figure 3 illustrates the formal topotactic condensation of the recently discovered high-pressure polymorph β-HPN_2 leading to β-HP_4N_7. The dashed lines indicate new connections formed during this process. During condensation half of the six-

Table 3. Selected Interatomic Distances/Å and Angles/deg in β-HP_4N_7

P1−N2	1.599(2)	P2−N1−P2	142.2(2)
P1−N3	1.568(2)	P1−N2−P2	136.2(2)
P1−N4	1.682(2)	P1−N3−P2	125.3(2)
P1−N4′	1.697(2)	P1−N4−P1	119.3(2)
P2−N1	1.560(2)	P1−N4−P2	123.3(2)
P2−N2	1.610(2)	P1−N4−P2′	117.3(2)
P2−N3	1.581(2)		
P2−N4	1.739(2)		
N2−H1	0.89(5)		
N2···H1	2.29(5)		

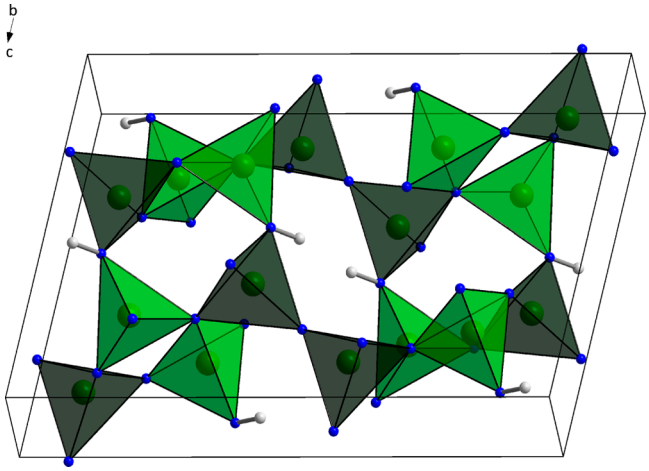

Figure 1. Crystal structure of β-HP_4N_7 in polyhedral representation (P1: light green, P2: dark green, N: blue, H: white).

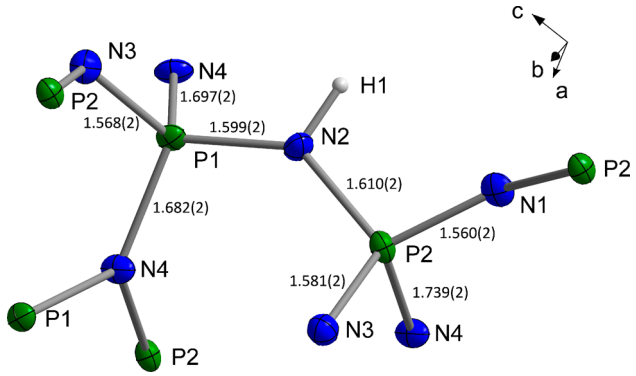

Figure 2. Atomic arrangement of P, N, H and bond lengths in β-HP_4N_7. Displacement ellipsoids are displayed at the 90% probability level.

Table 2. Atomic Coordinates and Isotropic Equivalent Displacement Parameters for β-HP_4N_7

atom	Wyckoff symbol	x	y	z	U_{iso}/Å^2	occupancy
P1	8f	0.18029(5)	0.2114(2)	0.22415(7)	0.0038(2)	1
P2	8f	0.10496(5)	0.3067(2)	−0.13583(7)	0.0041(2)	1
N1	4e	0	0.1987(6)	−1/4	0.0063(7)	1
N2	8f	0.1025(2)	0.1964(4)	0.0467(3)	0.0061(5)	1
N3	8f	0.1384(2)	0.3666(4)	0.3650(2)	0.0051(4)	1
N4	8f	0.2947(2)	0.3702(4)	0.2069(2)	0.0049(4)	1
H1	8f	0.051(4)	0.065(11)	0.035(9)	0.01(2)	0.5

dx.doi.org/10.1021/ic500767f | Inorg. Chem. 2014, 53, 7977−7982

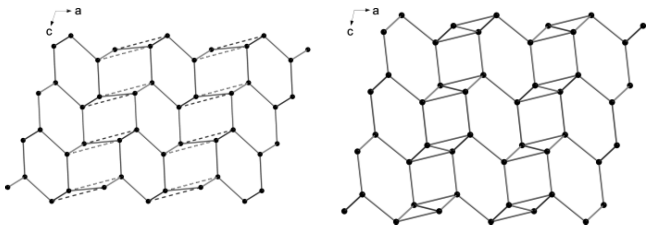

Figure 3. Topological relation between β-HPN_2 (left) and β-HP_4N_7 (right). Only P atoms (black spheres) are displayed for clarity. Each connecting line represents a P−N−P bond. New bonds formed by formal condensation are indicated by dashed lines.

membered rings are preserved, while the other half forms the 3- and 4-rings due to additional linkages.

In order to confirm the electrostatic consistency of the crystal structure, lattice energy calculations were performed using the MAPLE (Madelung part of lattice energy) software.[38] Both the overall and the partial MAPLE values for β-HP_4N_7, listed in Table 4, are in good agreement with those of the ambient

Table 4. Results of MAPLE Calculations for α-HP_4N_7 and β-HP_4N_7[a]

MAPLE value	α-HP_4N_7	β-HP_4N_7
overall	104 636	104 316
P atoms	15 691−17 079	16 054−16 814
$N^{[2]}$ atoms	5050−5679	4980−5498
$N^{[3]}$ atoms	6047−6163	6215

[a]All values are in kJ·mol^{-1}.

pressure polymorph. The small difference of 0.3% between both polymorphs confirms that the crystal structure of β-HP_4N_7 described here is electrostatically valid. All the partial MAPLE values for the atomic sites also fall in the range described in the literature.[5]

Powder X-ray Diffraction and Rietveld Refinement. In order to determine the bulk composition of the sample and evaluate the possible presence of side phases, a powder diffraction pattern was collected. Rietveld refinement was performed using the TOPAS-Academic package. The powder pattern and resulting difference curves are displayed in Figure 4. The refinement shows that the sample is composed of 89% β-HP_4N_7 and 11% crucible material BN. A few weak reflections could not be attributed to any known phase. Their position does not correspond to any possible superstructure of β-

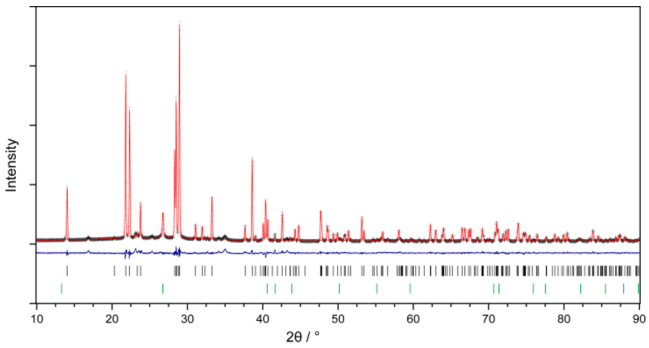

Figure 4. Observed (crosses) and calculated (red line) powder diffraction pattern of β-HP_4N_7 as well as position of Bragg reflections (black: β-HP_4N_7; green: BN) and difference profile (blue line).

HP_4N_7. Therefore, these peaks are likely due to small amounts of an unknown impurity. The refinement also confirms the structure determined by single-crystal structure analysis. Further details on the Rietveld refinement can be found in the Supporting Information. In order to ascertain the thermodynamic stability of β-HP_4N_7, high-temperature powder X-ray diffraction was performed. No phase transition could be determined up to the maximum temperature of 800 °C. This could suggest that β-HP_4N_7 could be the thermodynamically stable phase at ambient pressure. However, due to the large difference in densities, it is more likely that phase transition to the ambient pressure phase is kinetically hindered below 800 °C.

Spectroscopic Methods. Due to the fact that HP_4N_7 and P_4N_6O are isoelectronic, X-ray diffraction is insufficient to prove the identity of the title compound. In order to unequivocally determine the presence of hydrogen in the sample, FTIR and solid-state NMR spectroscopy were performed. As expected, the FTIR spectrum of β-HP_4N_7 (Figure 5) bears a strong similarity to that of α-HP_4N_7. The

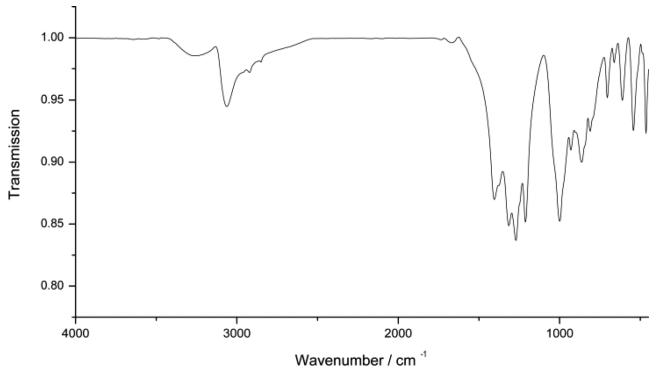

Figure 5. FTIR spectrum of β-HP_4N_7.

strong N−H stretching band at 3000 cm^{-1} shows that the sample contains significant amounts of imidic hydrogen (N−H groups). Further bands at 1050−1500 cm^{-1} and 600−1000 cm^{-1} correspond to P═N−P and P−NH−P asymmetric stretching modes, respectively.[31,39] Additional indication of the presence of stoichiometric amounts of hydrogen can be obtained from the ^{1}H solid-state NMR spectrum shown in Figure S1 in the Supporting Information.

Information about the local chemical environments of the P atoms can be derived from the ^{31}P solid-state NMR spectrum, which is displayed in Figure 6. The sample exhibits four distinct signals, which correspond to four different atomic environments. This seems to be contradictory with the fact that the single-crystal structure shows only two distinct P sites. However, this discrepancy can be explained by the nature of the H atom. Since only one of the two adjacent hydrogen sites can be occupied simultaneously, inversion symmetry is violated locally and the P sites split into four distinct atomic environments. Due to the extremely small influence of the hydrogen atom on the total electron density, the effect of this phenomenon is not detectable using X-ray crystallography. The chemical shifts of the signals (−11.8, −18.4, −24.6, −32.5 ppm) are close to the shift reported for α-HP_4N_7 and fall into the range expected for highly condensed nitridophosphates.

In order to gain insight into the gray color of the sample, the band gap of the sample was investigated using diffuse reflectance UV−vis spectroscopy. The Tauc plot (Figure S2)

dx.doi.org/10.1021/ic500767f | Inorg. Chem. 2014, 53, 7977−7982

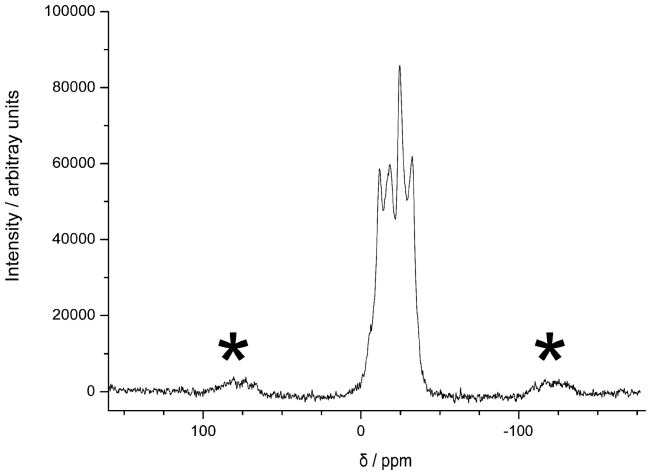

Figure 6. ^{31}P MAS NMR spectrum of β-HP_4N_7. Rotational sidebands are marked with asterisks.

shows that the band gap of β-HP_4N_7 is higher than 4.5 eV. Thus, the color of the sample is not intrinsic, but rather due to small amounts of a dark impurity.

CONCLUSION

A new polymorph of phosphorus nitride imide HP_4N_7 has been synthesized by reaction of P_3N_5 and NH_4Cl at high-pressure high-temperature conditions. We were able to thoroughly characterize the compound by means of single-crystal X-ray diffraction and FTIR and solid-state NMR spectroscopy. The compound crystallizes in an entirely new structure type with a framework topology that has not been observed so far. This structure consists of a three-dimensional framework of all-side vertex-sharing PN_4 tetrahedra. We could show that this structure can be derived from that of the high-pressure phase of HPN_2 by formal topotactic condensation. Considering the variety of different polymorphs in the closely related phosphorus oxonitride PON, the discovery of a phase transition in HP_4N_7 at moderate pressures could be indicative of the existence of further polymorphs at higher pressures. The structural flexibility displayed by HP_4N_7 makes it an interesting candidate for high-pressure synthesis of potential phases containing 5- or 6-fold-coordinated phosphorus.

ASSOCIATED CONTENT

Supporting Information

Crystallographic data in CIF format, table of anisotropic displacement parameters, full list of bond angles, details of the Rietveld refinement, and ^{1}H-MAS NMR spectrum. This material is available free of charge via the Internet at http://pubs.acs.org.

AUTHOR INFORMATION

Corresponding Author

*E-mail: wolfgang.schnick@uni-muenchen.de. Phone: (+49) 89-2180-77436. Fax: (+49)89-2180-77440.

Author Contributions

The manuscript was written through contributions of all authors. All authors have given approval to the final version of the manuscript.

Notes

The authors declare no competing financial interest.

REFERENCES

(1) (a) Taylor, D. *Mineral. Mag.* **1983**, *47*, 319−326. (b) Taylor, D. *Mineral. Mag.* **1984**, *48*, 65−79.
(2) Wilson, S. T.; Lok, B. M.; Messina, C. A.; Cannan, T. R.; Flanigen, E. M. *J. Am. Chem. Soc.* **1982**, *104*, 1146−1147.
(3) Mumpton, F. A. *Proc. Natl. Acad. Sci. U.S.A.* **1999**, *96*, 3463−3470.
(4) Beall, G. H. *Rev. Mineral* **1994**, *29*, 469−505.
(5) (a) Zeuner, M.; Pagano, S.; Schnick, W. *Angew. Chem.* **2011**, *123*, 7898−7920. (b) Zeuner, M.; Pagano, S.; Schnick, W. *Angew. Chem., Int. Ed.* **2011**, *50*, 7754−7775.
(6) (a) Baumann, D.; Sedlmaier, S. J.; Schnick, W. *Angew. Chem.* **2012**, *124*, 4785−4787. (b) Baumann, D.; Sedlmaier, S. J.; Schnick, W. *Angew. Chem., Int. Ed.* **2012**, *51*, 4707−4709.
(7) (a) Correll, S.; Oeckler, O.; Stock, N.; Schnick, W. *Angew. Chem.* **2003**, *115*, 3674−3677. (b) Correll, S.; Oeckler, O.; Stock, N.; Schnick, W. *Angew. Chem., Int. Ed.* **2003**, *42*, 3549−3552. (c) Correll, S.; Stock, N.; Oeckler, O.; Senker, J.; Nilges, T.; Schnick, W. *Z. Anorg. Allg. Chem.* **2004**, *630*, 2205−2217.
(8) Sedlmaier, S. J.; Döblinger, M.; Oeckler, O.; Weber, J.; Schmedt auf der Günne, J.; Schnick, W. *J. Am. Chem. Soc.* **2011**, *133*, 12069−12078.
(9) (a) Karau, F.; Schnick, W. *Angew. Chem.* **2006**, *118*, 4617−4620. (b) Karau, F.; Schnick, W. *Angew. Chem., Int. Ed.* **2006**, *45*, 4505−4508.
(10) (a) Grande, T.; Holloway, J. R.; McMillan, P. F.; Angell, C. A. *Nature* **1994**, *369*, 43−45. (b) Grande, T.; Jacob, S.; Holloway, J. R.; McMillan, P. F.; Angell, C. A. *J. Non-Cryst. Solids* **1995**, *184*, 151−154.
(11) Levchik, S. V.; Levchik, G. F.; Balabanovich, A. I.; Weil, E. D.; Klatt, M. *Angew. Makromol. Chem.* **1999**, *264*, 48−55.
(12) Weil, E. D.; Patel, N. G. *Fire Mater.* **1994**, *18*, 1−7.
(13) Ching, W. Y.; Aryal, S.; Rulis, P.; Schnick, W. *Phys. Rev. B: Condens. Matter Mater. Phys.* **2011**, *83*, 155109-1−155109-8.
(14) Neuhaus, A. *Chimia* **1964**, *18*, 93−103.
(15) Manjón, F. J.; Errandonea, D. *Phys. Status Solidi B* **2009**, *246*, 9−31.
(16) Sinclair, W.; Ringwood, A. E. *Nature* **1978**, *272*, 714−715.
(17) (a) Landskron, K.; Huppertz, H.; Senker, J.; Schnick, W. *Angew. Chem.* **2001**, *113*, 2713−2716. (b) Landskron, K.; Huppertz, H.; Senker, J.; Schnick, W. *Angew. Chem., Int. Ed.* **2001**, *40*, 2643−2645. (c) Landskron, K.; Huppertz, H.; Senker, J.; Schnick, W. *Z. Anorg. Allg. Chem.* **2002**, *628*, 1465−1471.
(18) Stock, A.; Grüneberg, H. *Ber. Dtsch. Chem. Ges* **1907**, *40*, 2573−2578.
(19) Huppertz, H. *Z. Kristallogr.* **2004**, *219*, 330−338.
(20) Kawai, N.; Endo, S. *Rev. Sci. Instrum.* **1970**, *41*, 1178−1181.
(21) Walker, D.; Carpenter, M. A.; Hitch, C. M. *Am. Mineral.* **1990**, *75*, 1020−1028.
(22) Walker, D. *Am. Mineral.* **1991**, *76*, 1092−1100.
(23) Rubie, D. C. *Phase Transitions* **1999**, *68*, 431−451.
(24) Palatinus, L.; Chapuis, G. *J. Appl. Crystallogr.* **2007**, *40*, 786−790.
(25) Oszlányi, G.; Sütő, A. *Acta Crystallogr., Sect. A: Found. Crystallogr.* **2005**, *61*, 147−152.
(26) Oszlányi, G.; Sütő, A. *Acta Crystallogr., Sect. A: Found. Crystallogr.* **2004**, *60*, 134−141.
(27) Sheldrick, G. M. *Acta Crystallogr., Sect. A: Found. Crystallogr.* **2008**, *64*, 112−122.
(28) Coelho, A. A. *TOPAS-Academic*, Version 4.1; Coelho Software: Brisbane, 2007.
(29) Bergmann, J.; Kleeberg, R.; Haase, A.; Breidenstein, B. *Mater. Sci. Forum* **2000**, *347−349*, 303−308.
(30) Cheary, R. W.; Coelho, A. A.; Cline, J. P. *J. Res. Natl. Inst. Stand. Technol.* **2004**, *109*, 1−35.
(31) (a) Horstmann, S.; Irran, E.; Schnick, W. *Angew. Chem.* **1997**, *109*, 2085−2087. (b) Horstmann, S.; Irran, E.; Schnick, W. *Angew. Chem., Int. Ed. Engl.* **1997**, *36*, 1992−1994. (c) Horstmann, S.; Irran, E.; Schnick, W. *Z. Anorg. Allg. Chem.* **1998**, *624*, 221−227.

(32) (a) Marchuk, A.; Pucher, F. J.; Karau, F. W.; Schnick, W. *Angew. Chem.* **2014**, *126*, 2501−2504. (b) Marchuk, A.; Pucher, F. J.; Karau, F. W.; Schnick, W. *Angew. Chem., Int. Ed.* **2014**, *53*, 2469−2472.
(33) Further details of the crystal structure investigation can be obtained from the Fachinformations-Zentrum Karlsruhe, 76344 Eggenstein-Leopoldshafen, Germany (fax: (+49)7247-808-666; e-mail: crysdata@fiz-karlsruhe.de) on quoting the depository number CSD-427230.
(34) Landskron, K.; Irran, E.; Schnick, W. *Chem.—Eur. J.* **1999**, *5*, 2548−2553.
(35) Blatov, V. A.; O'Keeffe, M.; Proserpio, D. M. *CrystEngComm* **2010**, *12*, 44−48.
(36) Blatov, V. A. *IUCr CompComm Newsletter* **2006**, *7*, 4−38.
(37) Ronis, J.; Bondars, B.; Vitola, A.; Millers, T.; Schneider, J.; Frey, F. *J. Solid State Chem.* **1995**, *115*, 265−269.
(38) (a) Hoppe, R. *Angew. Chem.* **1966**, *78*, 52−63; *Angew. Chem., Int. Ed. Engl.* **1966**, *5*, 95−106. (b) Hoppe, R. *Angew. Chem.* **1970**, *82*, 7−16; *Angew. Chem., Int. Ed. Engl.* **1970**, *9*, 25−34.
(39) Lücke, J.; Schnick, W. *Z. Anorg. Allg. Chem.* **1992**, *610*, 121−126.